An analysis of convection in a mushy layer with a deformable permeable interface

S. M. ROPER[1], S. H. DAVIS[1] AND P. W. VOORHEES[2]

[1]Engineering Sciences and Applied Math, Northwestern University, 2145 Sheridan Road, Evanston, IL 60208-3125, USA

[2]Materials Science and Engineering, Northwestern University, 2220 Campus Drive, Evanston, IL 60208-3108, USA

We study the dynamics of a mushy layer in directional solidification for the case of a thin near-eutectic mush with a deformable and permeable mush–liquid interface. We examine the onset of convection using linear stability analysis, and the weakly nonlinear growth of liquid inclusions that signal the onset of chimneys. This analysis is compared to past analyses in which the mush–liquid interface is replaced by a rigid impermeable lid. We find qualitative agreement between the two models, but the rigid-lid approximation gives substantially different quantitative behaviour.

In linear theory, the rigid-lid approximation leads to an over-estimate of the critical Rayleigh number and wavenumber of the instability. The condition for the onset of oscillatory instability is also changed by a factor of about 5 in composition number C. In the weakly nonlinear theory, the location of the onset of liquid inclusions is near the undisturbed front for the free-boundary analysis, whereas it lies at the centre of the mushy layer when the rigid-lid approximation is used. For hexagonal patterns, the boundary between regions of parameter space in which up and down hexagons are stable, shifts as a result of coupling between the liquid and mush regions.

1. Introduction

A mushy layer is a region of partially solidified melt, often with a complex dendritic structure. During the solidification of a multi-component alloy, a mushy layer forms as a result of a morphological instability (Mullins & Sekerka 1964) of the solidification front and undergoes a further instability if the buoyancy of the rejected components gives rise to an unstable density gradient in the mush. If the mush Rayleigh number

$$R_m = \frac{\rho_0 g \beta \Delta C \Pi^*}{V \nu} \qquad (1.1)$$

is larger than a critical value R_c, then the system undergoes a transition to convection (Worster 1992). The interaction of the convective fluid motions with the thermal field leads to solidification and dissolution of the mushy layer and can eventually lead to the formation of chimneys (Schulze & Worster 1999; Chung & Worster 2002). Chimneys affect the structure of the final solidified material as well as redistribute solute around the melt. As such, the processes which produce the chimneys are an important area of study in both metallurgy and geophysics.

The study of mushy-layer convection has evolved from formulations of the equations governing solidification and transport through the mush (Hills, Loper & Roberts 1983; Fowler 1985), for a review of mushy-layer convection and chimney

formation, see Worster (1997). The mechanisms for chimney growth are well understood as a result of upflow within the mush. The initial stages of chimney formation have been understood in terms of the bifurcation to convection (Amberg & Homsy 1993; Anderson & Worster 1995) and the further development from these weakly nonlinear solutions has been studied through various numerical approaches, charting the progress of the nonlinear convection until a liquid inclusion forms (Schulze & Worster 1999), to the development of chimneys (Chung & Worster 2002; Schulze & Worster 2005). In analytical treatments of mushy-layer convection, it has been common to make certain simplifications to render the analysis tractable and to allow elucidation of the physical mechanisms at play during the formation of chimneys (Amberg & Homsy 1993; Anderson & Worster 1995, 1996; Riahi 2002; Guba & Worster 2006). These assumptions are commonly that the mush–liquid interface is rigid and impermeable (Amberg & Homsy 1993; Anderson & Worster 1995) or rigid, but with a constant-pressure boundary condition (Chung & Chen 2000).

In weakly nonlinear analyses, a simplification often made is that the mush–liquid interface does not deform and is impermeable – the rigid-lid approximation. These two assumptions lead to very simple results for the structure of convection at onset and allow calculations to be performed that determine the nature of the bifurcation to convection. However, a detailed analytical study of these assumptions has not been undertaken.

In this paper, the equations governing mushy-layer convection in steady directional solidification with a deformable and permeable liquid–mush interface are studied to assess the effects of the rigid-lid assumption, employed in all previous analyses, and hence determine quantitative descriptions of the differences for comparison with experiments.

In §2, we review the equations that govern mushy-layer convection. Throughout this study, we use the near-eutectic approximation and the limit of large far-field temperature. The modes of convection when the thermal buoyancy in the liquid is large and small are explored in §3. In §4 we sketch the weakly nonlinear analysis and discuss the finite-amplitude solutions obtained. A concluding summary is given in §5 where we compare our results to experimental findings on the planforms of mushy-layer convection.

2. Equations

The equations used to describe mushy-layer convection are well established in the literature (e.g. Fowler 1985; Worster 1992; Amberg & Homsy 1993; Anderson & Worster 1995) and are presented here for completeness. Figure 1 outlines the situation: during directional solidification of a binary alloy, the temperature T and composition C of the liquid obey advection–diffusion equations in a frame fixed in the laboratory as the fluid is pulled down at speed V. The composition C is the composition of the less dense component of the alloy. The fluid velocity $\boldsymbol{u}$ obeys the Navier–Stokes equation in the liquid and Darcy's equation in the mush. Conservation of solute applies in the mush and it is assumed that the fluid in the mush is in local thermodynamic equilibrium with the solid, so that the temperature and composition are constrained by the liquidus relation $T = T_L(C)$ (Worster 1997). We assume that the thermophysical properties of the solid and liquid phases in the mush are the same, so that average properties of the mush are the same as for the individual solid and liquid phases.
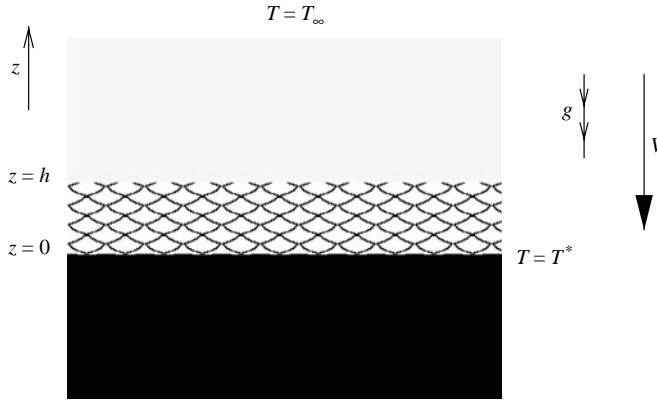
FIGURE 1. A sketch of the system. A binary alloy is pulled at speed V towards a cooled region. The temperature of the fluid as $z \to \infty$ is T_∞ and its far-field composition is C_0. At a temperature $T = T^*$, the fluid becomes completely solid and a partially solidified mush region extends over $T^* < T < T_i$, where T_i is the temperature at the mush–liquid interface

The mush is described by a solid fraction ϕ and a permeability $\Pi(\chi)$, where $\chi = 1 - \phi$ is the liquid fraction. The composition of the solid in the mush is C_s and we assume infinite back diffusion in the solid so that the lever rule can be applied. Remaining quantities that describe the system are the pressure p, the diffusivities of temperature κ and of composition D, the dynamic viscosity μ, the latent heat of fusion per kilogram L and the specific heat C_p. The density is $\rho(T, C)$ and a reference density is ρ_0. The Boussinesq approximation is made so that density variations are retained only in the buoyancy term in the Navier–Stokes equation. Gravity $\boldsymbol{g} = (0, 0, -g)$ points downwards, in the direction in which the sample is being pulled.

2.1. *Non-dimensionalization*

The non-dimensionalized equations for an ideal mushy layer with an overlying liquid layer are (from Worster 1992)

$$\frac{\partial \theta}{\partial t} - \frac{\partial \theta}{\partial z} + \boldsymbol{u} \cdot \nabla \theta = \nabla^2 \theta, \tag{2.1}$$

$$\frac{\partial \Theta}{\partial t} - \frac{\partial \Theta}{\partial z} + \boldsymbol{u} \cdot \nabla \Theta = \frac{1}{Le} \nabla^2 \Theta, \tag{2.2}$$

$$\frac{1}{\sigma} \left(\frac{\partial \boldsymbol{u}}{\partial t} - \frac{\partial \boldsymbol{u}}{\partial z} + \boldsymbol{u} \cdot \nabla \boldsymbol{u} \right) = R_T \theta z - R_C \Theta z - \mathscr{H} \nabla p + \nabla^2 \boldsymbol{u}, \tag{2.3}$$

in the liquid and

$$\frac{\partial \theta}{\partial t} - \frac{\partial \theta}{\partial z} + \boldsymbol{u} \cdot \nabla \theta = \nabla^2 \theta + \mathscr{S} \left(\frac{\partial \phi}{\partial t} - \frac{\partial \phi}{\partial z} \right), \tag{2.4}$$

$$\left(\frac{\partial}{\partial t} - \frac{\partial}{\partial z} \right) [(\mathscr{C} - \Theta)(1 - \phi)] + \boldsymbol{u} \cdot \nabla \Theta = \frac{1}{Le} \nabla^2 \Theta, \tag{2.5}$$

$$\theta = \Theta, \tag{2.6}$$

$$\boldsymbol{u} = -\Pi(\chi)(\nabla p + R_m \theta z), \tag{2.7}$$

in the mush. The non-dimensional temperature and composition are defined by

$$\theta = \frac{T - T_L(C_0)}{\Delta T}, \qquad \Theta = \frac{C_0 - C}{\Delta C}, \tag{2.8}$$

and non-dimensional fluid or Darcy velocity $\boldsymbol{u} = (u, v)$. Dimensional lengths have been scaled with κ/V, time with κ/V^2, velocities with V and pressure with $\kappa\mu/\Pi(0)$. The temperature scale is $\Delta T = T_L(C_0) - T_e$ and the composition scale is $\Delta C = C_e - C_0$, related by $\Delta T = -m\Delta C$, where m is the slope of the liquidus, T_e is the eutectic temperature and C_e is the eutectic composition. By virtue of the liquidus relationship, the equation of state in the mush becomes

$$\rho = \rho_0(1 + \beta\theta\Delta C), \tag{2.9}$$

where a new expansion coefficient is defined as $\beta = \beta^* + \alpha^* m$. The coefficient β takes into account the effects on density of temperature and composition, which are slaved in the mush by virtue of the liquidus relation. We can measure the importance of one of the factors over the other by considering the parameter $\mathscr{A} = -\alpha^* m/\beta$. The size of $\mathscr{A}$ determines whether the thermal buoyancy in the liquid is large enough to confine convective motion in the mushy layer.

The non-dimensional parameters that appear in (2.1)–(2.7) are the Lewis number $Le = \kappa/D$, Prandtl number $\sigma = \nu/\kappa$, thermal Rayleigh number $R_T = \rho_0\alpha^* \Delta T g \kappa^2/V^3\mu$ which can also be written $R_T = R_m\mathscr{H}\mathscr{A}$, solutal Rayleigh number $R_C = \rho_0\beta^*\Delta C g \kappa^2/V^3\mu = R_m\mathscr{H}(1 + \mathscr{A})$, inverse Darcy number $\mathscr{H} = \kappa^2/V^2\Pi(0)$, mush Rayleigh number $R_m = g\rho_0\beta\Delta C\Pi(0)/V\nu$, Stefan number $\mathscr{S} = L/C_p\Delta T$ and compositional number $\mathscr{C} = C_0/\Delta C$. We take $T \to T_\infty$ as $z \to \infty$, which gives another non-dimensional parameter $\theta_\infty = [T_\infty - T_L(C_0)]/\Delta T$.

2.2. *Boundary conditions*

To complete the specification of the problem, we must specify appropriate boundary conditions for the equations. The equations for θ are second order and so require two boundary conditions, together with continuity conditions across any interfaces,

$$\theta \to \theta_\infty \qquad \text{as } z \to \infty, \tag{2.10}$$

$$\theta = -1 \qquad \text{at } z = 0, \tag{2.11}$$

$$[\theta]_-^+ = 0 \qquad \text{at } z = h, \tag{2.12}$$

$$[\boldsymbol{n} \cdot \nabla\theta]_-^+ = 0 \qquad \text{at } z = h. \tag{2.13}$$

Similarly, for the concentration Θ, the equations are second order and require two boundary conditions. In the mush, the liquidus relationship $\Theta = \theta$ implies that the composition in the liquid is determined by the temperature θ. In the liquid, we require two boundary conditions for Θ, one of which is that it tends to its far-field value as $z \to \infty$, the other is extension of the liquidus relationship to the liquid side of the mush–liquid interface,

$$\Theta \to 0 \qquad \text{as } z \to \infty, \tag{2.14}$$

$$\theta = \Theta \qquad \text{at } z = h^+. \tag{2.15}$$

The condition of marginal stability, proposed in Worster (1986), determines the unknown interface location h,

$$\boldsymbol{n} \cdot \nabla\theta = \boldsymbol{n} \cdot \nabla\Theta \qquad \text{on the liquid side.} \tag{2.16}$$

The highest derivative of the solid fraction ϕ implies that we require one boundary condition to determine ϕ in the mushy layer. Conservation of solute leads us to deduce that $\phi = 0$ at the mush–liquid interface whenever flow is from the liquid into the mush (Schulze & Worster 1999).

The boundary conditions are modified when $Le \to \infty$, which is a singular perturbation of the equations. In that case, the condition of marginal stability is dropped and the interface location is determined by the liquidus constraint (2.15).

Mechanical boundary conditions, on the fluid velocity, are

$$\boldsymbol{u} \to \boldsymbol{0} \qquad \text{as } z \to \infty, \tag{2.17}$$

$$[\boldsymbol{u} \cdot \boldsymbol{n}]_-^+ = 0 \qquad \text{at } z = h, \tag{2.18}$$

$$\boldsymbol{u} - (\boldsymbol{u} \cdot \boldsymbol{n})\boldsymbol{n} = \boldsymbol{0} \qquad \text{at } z = h^+, \tag{2.19}$$

$$\boldsymbol{u} \cdot \boldsymbol{n} = 0 \qquad \text{at } z = 0, \tag{2.20}$$

$$[p]_-^+ = 0 \qquad \text{at } z = h. \tag{2.21}$$

These boundary conditions express mass continuity, no-slip on the liquid side of the mush–liquid interface, zero mass flow across the mush–solid interface and continuity of pressure across the mush–liquid interface.

The steady solution to (2.1)–(2.7), subject to these boundary conditions, and its stability to disturbances are characterized by the set of non-dimensional parameters $(Le, \mathscr{S}, \mathscr{C}, \theta_\infty, \mathscr{A}, \mathscr{H}, \sigma, R_m)$. The basic structure of the steady solution is of a horizontally uniform mushy layer, with an unstable density stratification in the mush and possibly in a compositional boundary layer in the liquid at the mush–liquid interface (e.g. Worster 1992). The thickness d of this boundary layer depends on Le and $d \to 0$ as $Le \to \infty$. The density contrast in the liquid is then a result of the stabilizing thermal field. In practice, the Lewis number Le is often very large and so we set $Le \to \infty$ for simplicity. In this paper, we are interested in the effects of the parameters $\mathscr{H}$ and $\mathscr{A}$ on the stability of the steady state in the limit of large θ_∞.

3. Limits

It has been shown (Amberg & Homsy 1993) that in the limit of large far-field temperature, the mushy layer is much thinner than the scale set by the pulling speed and thermal diffusion, κ/V. The non-dimensional mushy-layer depth in this case is given to leading order as

$$h = \delta \sim \frac{1}{\theta_\infty} \ll 1. \tag{3.1}$$

This result motivates a further rescaling of the variables. Following Amberg & Homsy (1993) and Anderson & Worster (1995), we remove any large effects of compositional changes on the solid fraction by assuming the compositional number is large $\mathscr{C} = \bar{C}/\delta$ and that therefore the solid fraction is $\phi \sim O(\delta)$, from (2.5). Similarly, we can retain the effects of latent heat by scaling the Stefan number $\mathscr{S} = \bar{S}/\delta$. We scale all lengths with the leading-order mush depth δ and time with δ^2.

3.1. *Steady-state and disturbance equations*

The steady state can be found straightforwardly from (2.1)–(2.5). It can be shown (e.g. Worster 1992) that in the limit of $Le \to \infty$, the temperature field in the liquid is

$$\theta_B = \theta_\infty \big(1 - e^{-(z-1)\delta}\big), \tag{3.2}$$

where the mush–liquid interface now lies at $z = 1$ at leading order. For values of z less than $O(\delta^{-1})$, an appropriate expansion is

$$\theta_B = (z - 1) + O(\delta). \tag{3.3}$$

In the mush, the steady conductive state is given by (e.g. Amberg & Homsy 1993; Anderson & Worster 1995)

$$\theta_B = \theta_{B0} + \delta\theta_{B1} + \cdots = (z-1) - \delta\tfrac{1}{2}\Omega(z^2 - z) + \cdots, \tag{3.4}$$

$$\phi_B = \delta\phi_{B0} + \delta^2\phi_{B1} = -\delta\frac{z-1}{\bar{C}} + \delta^2\left(-\frac{(z-1)^2}{\bar{C}^2} + \frac{\Omega}{2\bar{C}}(z^2 - z)\right) + \cdots, \tag{3.5}$$

where higher-order terms in δ can be easily calculated. The constant $\Omega = 1 + \bar{S}/\bar{C}$ combines the effects of latent heat and composition.

The governing equations are expanded to derive equations for small disturbances to the basic state. We seek, for the moment, the onset of steady convection and so set the complex growth rate of normal modes to be zero. We examine two cases, one in which $\mathscr{A}$ is effectively zero, and the other in which $\mathscr{A}$ is non-zero and plays a role in determining the critical Rayleigh number. We are primarily interested in rolls and so study only the two-dimensional disturbances in which there is no variation in the y-direction; this will be relaxed to study hexagonal patterns. We take the inverse Darcy number $\mathscr{H}$ to be large, which is a good approximation in many practical circumstances.

Make a double expansion in small amplitude ϵ and δ for the disturbances

$$\begin{aligned}\theta = \theta_B + \epsilon(\theta_{00} + \delta\theta_{01} + \cdots) + \epsilon^2(\theta_{10} + \delta\theta_{11} + \cdots)\\ + \epsilon^3(\theta_{20} + \delta\theta_{21} + \cdots) + o(\epsilon^3),\end{aligned} \tag{3.6}$$

$$\begin{aligned}\Theta = \Theta_B + \epsilon(\Theta_{00} + \delta\Theta_{01} + \cdots) + \epsilon^2(\Theta_{10} + \delta\Theta_{11} + \cdots)\\ + \epsilon^3(\Theta_{20} + \delta\Theta_{21} + \cdots) + o(\epsilon^3),\end{aligned} \tag{3.7}$$

$$\begin{aligned}\phi = \phi_B + \epsilon(\phi_{00} + \delta\phi_{01} + \cdots) + \epsilon^2(\phi_{10} + \delta\phi_{11} + \cdots)\\ + \epsilon^3\left(\frac{1}{\delta}\phi_{2(-1)} + \phi_{20} + \cdots\right) + o(\epsilon^3),\end{aligned} \tag{3.8}$$

$$\begin{aligned}\delta w = \epsilon(w_{00} + \delta w_{01} + \cdots) + \epsilon^2(w_{10} + \delta w_{11} + \cdots)\\ + \epsilon^3(w_{20} + \delta w_{21} + \cdots) + o(\epsilon^3),\end{aligned} \tag{3.9}$$

$$\begin{aligned}\delta u = \epsilon(u_{00} + \delta u_{01} + \cdots) + \epsilon^2(u_{10} + \delta u_{11} + \cdots)\\ + \epsilon^3(u_{20} + \delta u_{21} + \cdots) + o(\epsilon^3),\end{aligned} \tag{3.10}$$

$$\delta R_m = R^2 + \epsilon R_1 + \epsilon^2 R_2 + \cdots, \tag{3.11}$$

$$\begin{aligned}h = h_B + \epsilon(h_{00} + \delta h_{10} + \cdots) + \epsilon^2(h_{10} + \delta h_{11} + \cdots)\\ + \epsilon^3(h_{20} + \delta h_{21} + \cdots) + o(\epsilon^3).\end{aligned} \tag{3.12}$$

3.2. *Expansion of equations*

As a result of expansions (3.6)–(3.12) and using (3.3)–(3.5) for the basic state, the governing equations at $O(\epsilon^1\delta^0)$ become

$$\bar{S}\frac{\partial\phi_{00}}{\partial z} + w_{00} = \nabla^2\theta_{00}, \tag{3.13}$$

$$-\bar{C}\frac{\partial\phi_{00}}{\partial z} + w_{00} = 0, \tag{3.14}$$

$$\nabla^2 w_{00} + R^2\nabla_H^2\theta_{00} = 0, \tag{3.15}$$

in the mush, and

$$w_{00} = \nabla^2 \theta_{00}, \tag{3.16}$$

$$\nabla^4 w_{00} + \mathcal{H}\mathcal{A}R^2\delta^2\nabla_H^2\theta_{00} + \frac{\delta}{\sigma}\frac{\partial}{\partial z}\nabla^2 w_{00} = 0, \tag{3.17}$$

in the liquid, where we have retained some terms involving δ to deduce the conditions on the other parameters. The boundary conditions at this order are

$$\theta_{00} \to 0 \qquad \text{as } z \to \infty, \tag{3.18}$$

$$\theta_{00} = 0 \qquad \text{at } z = 0, \tag{3.19}$$

$$[\theta_{00}]_-^+ = 0 \qquad \text{at } z = 1, \tag{3.20}$$

$$\left[\frac{\partial \theta_{00}}{\partial z}\right]_-^+ = 0 \qquad \text{at } z = 1, \tag{3.21}$$

$$h_{00} + \theta_{00}(1^+) = 0, \tag{3.22}$$

and

$$w_{00} \to 0 \qquad \text{as } z \to \infty, \tag{3.23}$$

$$[w_{00}]_-^+ = 0 \qquad \text{at } z = 1, \tag{3.24}$$

$$u_{00} = 0 \qquad \text{at } z = 1^+, \tag{3.25}$$

$$w_{00} = 0 \qquad \text{at } z = 0, \tag{3.26}$$

$$\frac{\partial w_{00}}{\partial z}(1^-) = -\frac{1}{\mathcal{H}\delta^2}\left(\frac{\partial \nabla^2 w_{00}}{\partial z} + \frac{\delta}{\sigma}\frac{\partial^2 w_{00}}{\partial z^2}\right)(1^+), \tag{3.27}$$

where the last of these represents continuity of pressure across the mush–liquid interface. Finally, the boundary condition on ϕ is

$$\phi_{00} = 0 \qquad \text{at } z = 1. \tag{3.28}$$

Higher-order expansions in ϵ are required in order to study the weakly nonlinear development of instabilities. The equations and boundary conditions at $O(\epsilon^2)$ and $O(\epsilon^3)$ are given in the Appendix.

3.3. *Solution at $O(\epsilon)$*

Using (3.13)–(3.17) and further setting

$$\theta_{00} = e^{ikx}\hat{\theta}, \qquad \phi_{00} = e^{ikx}\hat{\phi}, \qquad w_{00} = e^{ikx}\hat{w}, \qquad u_{00} = \frac{1}{ik}e^{ikx}\hat{w}', \qquad h_{00} = e^{ikx}\hat{h} \tag{3.29}$$

so that for the liquid region at $O(\epsilon^1\delta^0)$ the disturbance equations become, with $D_z = d/dz$,

$$D_z^2\hat{\theta} - k^2\hat{\theta} - \hat{w}D_z\theta_{B0} = 0, \tag{3.30}$$

$$\left(D_z^2 - k^2\right)^2\hat{w} - \delta^2k^2\mathcal{A}\mathcal{H}R^2\hat{\theta} + \frac{\delta}{\sigma}\left(D_z^3 - k^2D_z\right)\hat{w} = 0. \tag{3.31}$$

If σ is $O(1)$ and $\mathcal{A}\mathcal{H}$ is $o(\delta^{-1})$, then (3.30) and (3.31) simplify further. In the mush at $O(\epsilon^1\delta^0)$,

$$D_z^2\hat{\theta} - k^2\hat{\theta} + \bar{S}D_z\hat{\phi} - \hat{w} = 0, \tag{3.32}$$

$$-\bar{C}D_z\hat{\phi} + \hat{w} = 0, \tag{3.33}$$

$$\left(D_z^2 - k^2\right)\hat{w} = R^2k^2\hat{\theta}, \tag{3.34}$$

where it has been assumed that $\Pi(\chi) \equiv 1$ in Darcy's equation so that there are no effects of porosity-dependent permeability.

Boundary conditions are $\hat{\theta}(0) = \hat{w}(0) = 0$, $\hat{w}'(1^+) = 0$ (no slip at liquid–mush interface), $\hat{w}(\infty) = 0$ and $\theta(\infty) = 0$. The quantities $\hat{\theta}$ and $\hat{w}$ are continuous at $z = 1$. Continuity of pressure at the interface gives the following condition on $\hat{w}$

$$D_z \hat{w}(1^-) = -\frac{1}{\mathscr{H}\delta^2} \left(D_z^3 - k^2 D_z + \frac{\delta}{\sigma} D_z^2 \right) \hat{w}(1^+); \qquad (3.35)$$

we also have the following boundary condition from the continuity of thermal flux

$$D_z \hat{\theta}(1^+) = D_z \hat{\theta}(1^-). \qquad (3.36)$$

Finally, the condition on the solid fraction leads to the boundary condition

$$\hat{\phi} = 0 \qquad \text{at } z = 1, \qquad (3.37)$$

and the interface location is determined by (3.22) so

$$\hat{h} = -\hat{\theta}(1). \qquad (3.38)$$

This set of equations and boundary conditions describe the onset of convection. We can explore the structure of the convecting modes at onset in different limits of the parameters $\mathscr{A}$ and $\mathscr{H}$.

3.4. *Stabilizing thermal buoyancy is zero: $\mathscr{A} = 0$*

In the case $\mathscr{A} = 0$ and $\sigma = O(1)$, the disturbance equations in the liquid region, to leading order in δ, are

$$D_z^2 \hat{\theta} - k^2 \hat{\theta} = \hat{w}, \qquad (3.39)$$

$$\left(D_z^2 - k^2 \right)^2 \hat{w} = 0, \qquad (3.40)$$

and in the mushy region, eliminating the solid fraction $\hat{\phi}$ from (3.32) and (3.33),

$$D_z^2 \hat{\theta} - k^2 \hat{\theta} = \Omega \hat{w}, \qquad (3.41)$$

$$D_z^2 \hat{w} - k^2 \hat{w} = R^2 k^2 \hat{\theta}. \qquad (3.42)$$

Boundary conditions are $\hat{\theta}(0) = \hat{w}(0) = 0$, $\hat{w}'(1^+) = 0$, $\hat{w}(\infty) = 0$ and $\hat{\theta}(\infty) = 0$. The quantities $\hat{\theta}$, $\hat{\theta}'$ and $\hat{w}$ are continuous at $z = 1$. Application of the condition of continuity of pressure gives $\hat{w}'(1^-) = 0$ as long as $\mathscr{H}^{-1}$ is $O(\delta^3)$. The solution for $\hat{w}$ in the liquid region is

$$\hat{w} = a_0 e^{k(z-1)} + b_0 e^{-k(z-1)} + a_1(z-1)e^{k(z-1)} + b_1(z-1)e^{-k(z-1)}, \qquad (3.43)$$

where a_0, a_1, b_0 and b_1 are integration constants. Upon application of the boundary conditions,

$$\hat{w} = W_1(1 + k(z-1))e^{-k(z-1)}. \qquad (3.44)$$

for $z \geqslant 1$, where W_1 is an integration constant. Similarly, from (3.39) and the remaining boundary condition at infinity, the temperature $\hat{\theta}$ is

$$\hat{\theta} = T_1 e^{-k(z-1)} - \frac{W_1}{4k}(z-1)(3 + k(z-1))e^{-k(z-1)}. \qquad (3.45)$$

for $z \geqslant 1$, where T_1 is an integration constant. Continuity of $\hat{w}$, $\hat{\theta}$ and $\hat{\theta}'$ across the interface leaves us with an eigenvalue problem for R and for the quantities in the
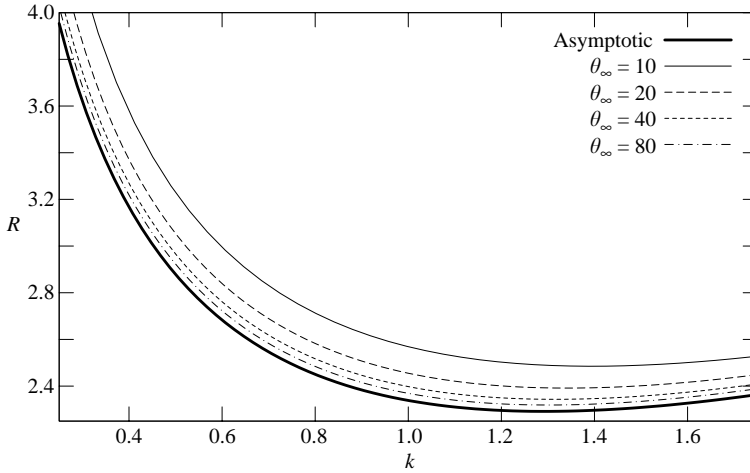
FIGURE 2. Plot of scaled critical Rayleigh number R against disturbance wavenumber k for $\Omega = 2$ (from $C = 1$ and $S = 1$), $\mathcal{H}\delta^2 = 10^5$ and $\sigma = 2$. The value of $\mathcal{H}$ is adjusted so as to maintain the validity of $w'(1^-) = 0$ as an approximation to boundary condition (3.35). The error is order δ, as expected.

mushy region, with the following boundary conditions

$$\hat{\theta}(0) = 0, \qquad \hat{w}(0) = 0, \qquad \hat{w}'(1) = 0, \qquad \hat{\theta}'(1) + k\hat{\theta}(1) + \frac{3}{4k}\hat{w}(1) = 0. \qquad (3.46)$$

The solution to (3.41) and (3.42) with boundary conditions (3.46) is

$$\hat{w} = A \sinh(m_r z) + B \sin(m_i z), \qquad (3.47)$$

$$\hat{\theta} = \frac{\sqrt{\Omega}}{Rk}[A \sinh(m_r z) - B \sin(m_i z)], \qquad (3.48)$$

for $0 \leqslant z \leqslant 1$, where $m_r^2 = Rk\sqrt{\Omega} + k^2$, $m_i^2 = Rk\sqrt{\Omega} - k^2$ and A and B are constants of integration. Using the boundary conditions, we derive a condition on the following determinant for the existence of non-trivial solutions

$$\begin{vmatrix} \sqrt{\Omega}(m_r \cosh m_r + k \sinh m_r) + \dfrac{3R}{4}\sinh m_r & m_r \cosh m_r \\ -\sqrt{\Omega}(m_i \cos m_i + k \sin m_i) + \dfrac{3R}{4}\sin m_i & m_i \cos m_i \end{vmatrix} = 0. \qquad (3.49)$$

When the determinant of the matrix is zero the scaled Rayleigh number R is at the marginal stability boundary. Marginal stability curves, derived from the determinant conditions and from full numerical calculations based on Worster (1992) and Chen, Lu & Chang (1994), are shown in figure 2. The figure shows good agreement between the numerical solutions and the asymptotic solution for large θ_∞ (and hence small δ). For each of the values of θ_∞ shown, the value of $\mathcal{H}$ varies so as to keep $\mathcal{H}\delta^2$ constant. If this is not the case, then boundary condition (3.35) has an increasing effect on the results as θ_∞ increases. Figure 3 shows the streamlines for the minimum R in the marginal stability curve in figure 2. The figure shows that there is significant flow in the liquid as well as the mush. The streamlines in the mush are very similar to $\Psi \sim \sin(kx)\sin(\pi z/2)$ and a possible simplification of the boundary conditions in the
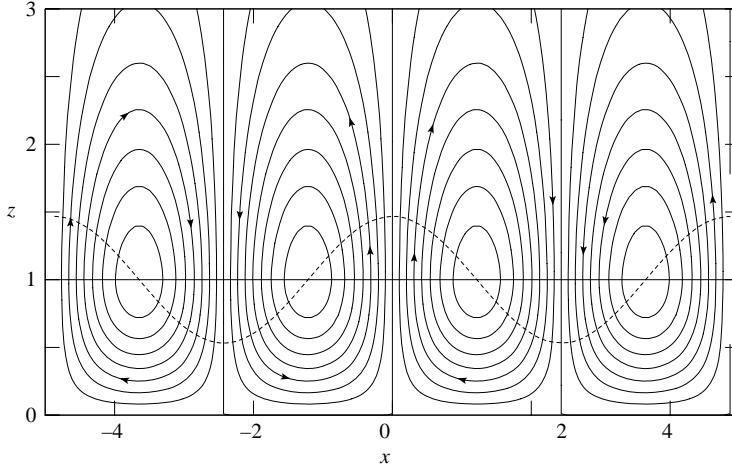
FIGURE 3. The form of the streamlines for $\Omega = 2$, $\mathcal{H} = 10^5$, $\sigma = 2$, $\mathcal{A} = 0$ and $\theta_\infty = 10$. The flow extends into the liquid. As expected, in this case the rigid-lid assumption fails to capture the form of the streamlines, the critical Rayleigh number and wavenumber. The interface shape is also shown (dotted), the magnitude of the deflection is determined by the amplitude of the convection and cannot be determined by linear theory.

case of small $\mathcal{A}$ would appear to be $\hat{\theta}' = 0$ and $\hat{w}' = 0$ at $z = 1$, leading to half-rolls as shown.

If the Prandtl number σ is not $O(1)$ but is instead $O(\delta)$, so that $\Sigma = \sigma/\delta$ is $O(1)$, the result does not change substantially. The solution in the liquid becomes

$$\hat{w} = W_\sigma \frac{(k^* e^{-k(z-1)} - k e^{-k^*(z-1)})}{k^* - k}, \tag{3.50}$$

$$\hat{\theta} = T_\sigma e^{-k(z-1)} - \frac{W_\sigma k \left(e^{-k^* z} - e^{-kz} \right)}{(k^* - k)(k^{*2} - k^2)} - \frac{W_\sigma k^* z e^{-k(z-1)}}{2k(k^* - k)}, \tag{3.51}$$

where $k^* = (2\Sigma)^{-1} + (k^2 + (4\Sigma^2)^{-1})^{1/2}$ and T_σ and W_σ are constants of integration.

The solution in the liquid changes one of the boundary conditions in (3.46) to

$$\hat{\theta}'(1) + k\hat{\theta}(1) + \frac{2k^* + k}{2k(k^* + k)} \hat{w}(1) = 0, \tag{3.52}$$

in the limit as $\Sigma \to \infty$, or equivalently $k^* \to k$, the solutions already obtained for the case when σ is $O(1)$ appear.

3.5. *Stabilizing buoyancy is large: $\mathcal{A} = O(1)$*

In the case where the fluid has large stabilizing buoyancy, the lengthscale of decay of the convective motion in the liquid becomes much smaller than the depth of the mush. We can simplify the governing equations to take this into account. Define a new constant $\Omega^* = \mathcal{H}\mathcal{A}\delta^2$ and assume that $\Omega^* \gg 1$. Then, the governing equations in the liquid become, to a first approximation

$$D_z^4 \hat{w} = R^2 k^2 \Omega^* \hat{\theta}, \tag{3.53}$$

$$D_z^2 \hat{\theta} = \hat{w}, \tag{3.54}$$

and in the mush they remain (3.41) and (3.42). The boundary conditions are $\hat{w} = \hat{\theta} = 0$ at $z = 0$, $\hat{w}$ is continuous at $z = 1$, $w \to 0$ and $\theta \to 0$ as $z \to \infty$, $\hat{\theta}$ and $\hat{\theta}'$ are continuous

at $z = 1$ and finally, continuity of pressure becomes

$$D_z \hat{w}|_{mush} = -\frac{\mathscr{A}}{\Omega^*} D_z^3 \hat{w}|_{liquid}. \tag{3.55}$$

The boundary conditions on $\hat{\phi}$ and $\hat{h}$ are the same as the case when $\mathscr{A} = 0$. In the liquid, the solution is

$$\hat{w} = A_{\mathscr{A}} e^{-\lambda(z-1)} + e^{-\lambda(z-1)/2} \left(B_{\mathscr{A}} \cos\left[\frac{\sqrt{3}\lambda}{2}(z-1) \right] + C_{\mathscr{A}} \sin\left[\frac{\sqrt{3}\lambda}{2}(z-1) \right] \right), \tag{3.56}$$

$$\hat{\theta} = \frac{A_{\mathscr{A}}}{\lambda^2} e^{-\lambda(z-1)} - \frac{1}{2\lambda^2} e^{-\lambda(z-1)/2} \left((B_{\mathscr{A}} - C_{\mathscr{A}}\sqrt{3}) \cos\left[\frac{\sqrt{3}\lambda}{2}(z-1) \right] \right.$$
$$\left. + (C_{\mathscr{A}} + B_{\mathscr{A}}\sqrt{3}) \sin\left[\frac{\sqrt{3}\lambda}{2}(z-1) \right] \right), \tag{3.57}$$

where $A_{\mathscr{A}}$, $B_{\mathscr{A}}$ and $C_{\mathscr{A}}$ are constants of integration. In the mush,

$$\hat{w} = D_{\mathscr{A}} \sinh(m_r z) + E_{\mathscr{A}} \sin(m_i z), \tag{3.58}$$

where $\lambda = (R^2 k^2 \Omega^*)^{1/6}$, $m_r^2 = Rk\sqrt{\Omega} + k^2$, $m_i^2 = Rk\sqrt{\Omega} - k^2$ and $D_{\mathscr{A}}$ and $E_{\mathscr{A}}$ are constants of integration. The temperature $\hat{\theta}$ is found using (3.41). Application of $\hat{w}'(1^+) = 0$ gives $C = (2A + B)/\sqrt{3}$. The continuity conditions across the mush–liquid interface lead once again to a linear system and for non-trivial solutions

$$\begin{vmatrix} 1 & 1 & -\sinh m_r & -\sin m_i \\ \mathscr{A}\lambda^3/\Omega^* & -\mathscr{A}\lambda^3/\Omega^* & -m_r \cosh m_r & -m_i \cos m_i \\ 2R/\lambda^2 & 0 & -\sqrt{\Omega} \sinh m_r/k & \sqrt{\Omega} \sin m_i/k \\ 2R/\lambda & R/\lambda & \sqrt{\Omega} m_r \cosh m_r/k & -\sqrt{\Omega} m_i \cos m_i/k \end{vmatrix} = 0. \tag{3.59}$$

The marginal stability curves derived from both the asymptotics and numerical solutions, for $\mathscr{A} = 1$, $\mathscr{H} = 10^6$, $\Omega = 2$ and $\theta_\infty = 10$ are shown in figure 4. Also shown is the marginal stability curve under the assumption of a rigid-lid at which $\hat{w} = 0$ and $\hat{\theta} = 0$. This approximation is often employed in weakly nonlinear analyses of mushy-layer convection, as discussed in § 1. Although it renders the analysis much simpler in many circumstances, it is clear that it does not capture the full behaviour at the onset of convection. The streamlines in figure 5 are those calculated from the asymptotic solution and show that the convection is largely confined to the mush. Note that with a rigid impermeable lid, complete rolls are the form of the solution in the mush, whereas here they are partial rolls. This parameter regime corresponds to the case in which the boundary condition at the mush–liquid interface can be approximated as a constant-pressure boundary condition. Chung & Chen (2000) have performed the linear and weakly non-linear analysis of this case using the simplification of constant pressure applied at $z = 1$ when the mush–liquid interface is not deformable. They approximate the boundary conditions for the linear problem as $\hat{w}' = 0$ and $\hat{\theta} = 0$ at $z = 1$. Figure 4 shows the results of Chung & Chen (2000) compared with our analysis and compared with numerical results using the parameters relevant to the experiments of Tait, Jahrling & Jaupart (1992), given in Chen *et al.* (1994). Both the simplified boundary conditions used by Chung & Chen (2000) and our analysis give good agreement with the numerical results, and as δ is decreased our analysis captures the behaviour increasingly well with decreasing δ. It can be seen from figure 4 that
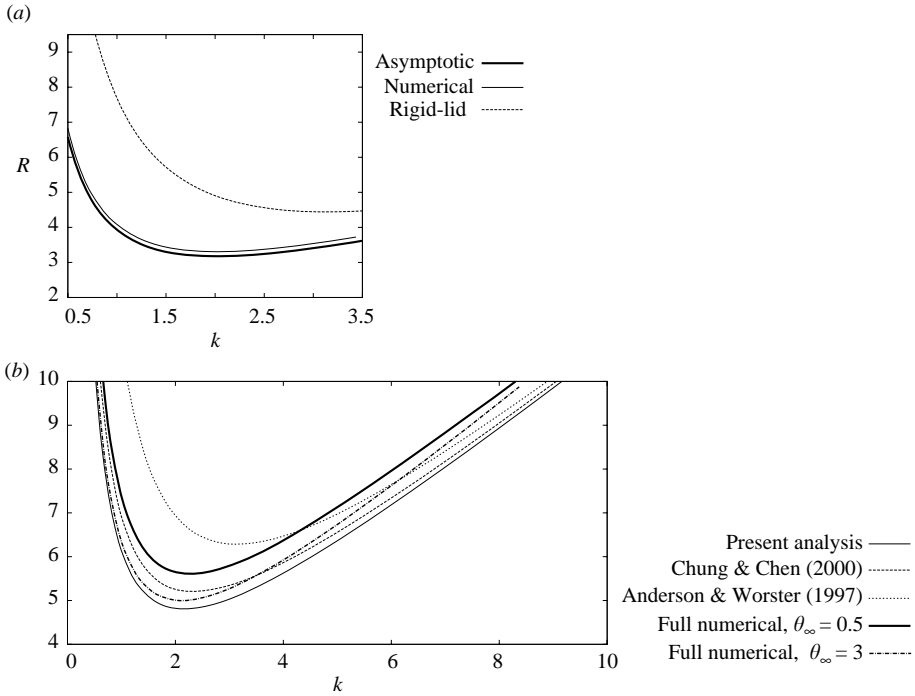
FIGURE 4. (a) The marginal stability curves for $\Omega = 2$, $\sigma = 2$, $\mathcal{A} = 1$ and $\mathcal{H} = 10^6$. The curves are derived from the asymptotic analysis presented here and from numerical integration of the full equations, using the numerical methods of Worster (1992) and Chen *et al.* (1994). The results in the case of a rigid-lid are shown for comparison. (b) Marginal stability curves using the various models for $\mathcal{C} = 12.3$, $\mathcal{S} = 3.2$, $\mathcal{H} = 3.5 \times 10^6$, $\sigma = 10$, $Le^{-1} = 0$, $\mathcal{A} = 0.65$ and $\theta_\infty = 0.5, 3$. The results of Chung & Chen (2000) and the present analysis compare well with the full numerical calculations. The rigid-lid calculation is also shown. The parameters represent experiments by Tait *et al.* (1992).

the inclusion of a deformable interface leads to a destabilization of the mushy layer with respect to the results of Chung & Chen (2000) and the rigid-lid assumption.

Figure 6 shows a comparison between the structure of the eigenfunction $\hat{w}(z)$ obtained numerically using the method of Worster (1992) and Chen *et al.* (1994) and the asymptotic analysis presented here. The agreement is very good and we expect errors of order δ.

4. Weakly nonlinear analysis

In this section, we confirm the assertion by Anderson & Worster (1996), that an oscillatory instability can occur as a result of compositional convection and solidification in the mush, even when the deformability of the mush–liquid interface and the hydrodynamics of the liquid are considered. We perform a weakly nonlinear analysis of the full two-layer model of convection in the same limits as the marginal stability calculation described above. The analysis is extremely complicated and we present an abbreviated version to outline the major steps in the calculation. We restrict our study to the case where $\mathcal{A} = 0$, though the approach taken can be used to study cases where $\mathcal{A} \neq 0$. In general, the problem is defined by a linear operator $\mathcal{L}$ and boundary conditions $\mathcal{B}_n$ acting upon variables v_n, where n refers to the order.
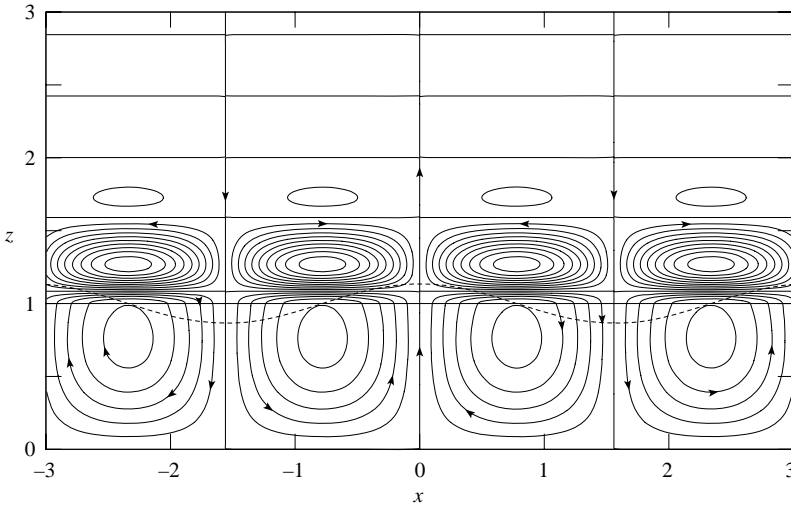
FIGURE 5. The form of the streamlines for $\Omega = 2$, $\mathcal{H} = 10^6$, $\sigma = 2$, $\mathcal{A} = 1$ and $\theta_\infty = 10$. The flow is confined by the thermal buoyancy in the liquid region. The interface deflection (dotted) is shown, though its amplitude cannot be determined by linear theory.
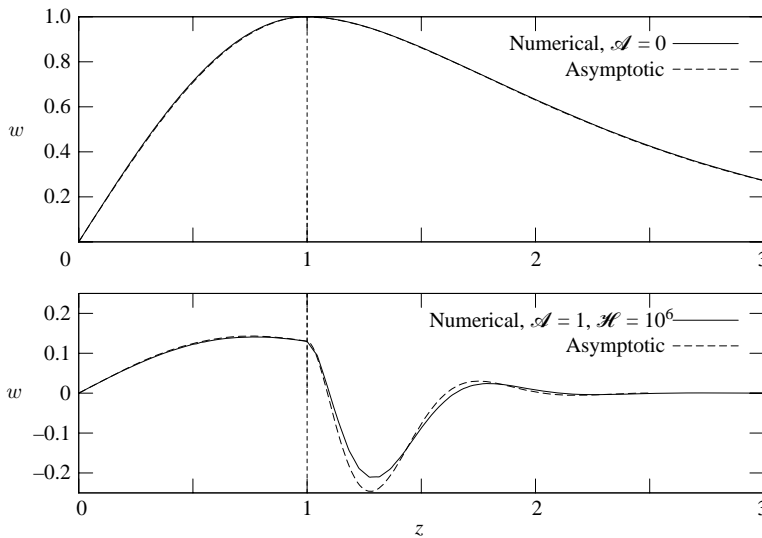

FIGURE 6. A comparison between the numerical and asymptotic profiles of vertical velocity component. The far-field temperature is $\theta_\infty = 10$, the errors are small (we expect relative errors of order δ). The scale for the velocity is arbitrary since these are calculations from linear stability. The mush–liquid interface lies at $z = 1$ (short dashed line).

The solution to the sequence of problems

$$\mathscr{L}v_1 = 0, \qquad \mathscr{B}_1(v_1) = 0, \tag{4.1}$$

$$\mathscr{L}v_2 = f_1(v_1), \qquad \mathscr{B}_2(v_2) = b_1(v_1), \tag{4.2}$$

$$\mathscr{L}v_3 = f_2(v_1, v_2), \qquad \mathscr{B}_3(v_3) = b_2(v_1, v_2), \tag{4.3}$$

plus the compatibility condition at $O(\epsilon^3)$,

$$\int_D v_1^\dagger \mathscr{L} v_3 \, \mathrm{d}V = J(v_1, v_2), \tag{4.4}$$

produces an amplitude equation for the unknown amplitude $A(\tau)$ of v_1 as a function of the slow time variable $\tau = \epsilon^2 t$. The function J represents boundary terms from the non-homogenous boundary conditions $\mathscr{B}_3$. In general, ignoring slow spatial modulations, the equation has the form

$$\bar{\tau}\frac{\mathrm{d}A}{\mathrm{d}\tau} = R_2 A - \lambda A |A|^2, \tag{4.5}$$

where the amplitude A is such that

$$w = A(\tau)\cos(kx)\bar{w}(z), \tag{4.6}$$

and where $\bar{w}$ is the solution to the linear stability problem at the onset of convection with the additional condition $\bar{w}(1) = 1$.

In order to execute this solution procedure, we must find the adjoint operator and boundary conditions. The adjoint problem in our case is give by the following equations, in the mush

$$\left(\mathrm{D}_z^2 - k^2\right)\tilde{w} = \Omega\tilde{\theta}, \tag{4.7}$$

$$\left(\mathrm{D}_z^2 - k^2\right)\tilde{\theta} = R^2 k^2 \tilde{w}, \tag{4.8}$$

and in the liquid

$$\left(\mathrm{D}_z^2 - k^2\right)\tilde{\theta} = 0, \tag{4.9}$$

$$\left(\mathrm{D}_z^2 - k^2\right)^2 \tilde{w} = \tilde{\theta}, \tag{4.10}$$

with adjoint boundary conditions $\tilde{\theta}(0) = 0$, $\tilde{w}(0) = 0$, $\tilde{w} \to 0$ and $\tilde{\theta} \to 0$ as $z \to \infty$, $\tilde{\theta}(1^+) - \tilde{\theta}(1^-) = \tilde{\theta}'(1^+) = \tilde{\theta}'(1^-) = 0$, $\tilde{w}(1^+) = 0$, $\tilde{w}'(1^+) = 0$ and $\tilde{w}'''(1^+) = \tilde{w}(1^-)$. The solution of the adjoint problem in the liquid is

$$\tilde{\theta} = T_a \mathrm{e}^{-k(z-1)}, \tag{4.11}$$

$$\tilde{w} = \frac{T_a}{8k^2}(z-1)^2 \mathrm{e}^{-k(z-1)}, \tag{4.12}$$

and in the mush

$$\tilde{\theta} = A_a \sinh(m_r z) + B_a \sin(m_i z), \tag{4.13}$$

$$\tilde{w} = \frac{\sqrt{\Omega}}{Rk}(A_a \sinh(m_r z) - B_a \sin(m_i z)), \tag{4.14}$$

where m_r and m_i have the same definitions as in §3. The constants are linearly related through application of boundary conditions, and for a non-trivial solution we derive the same condition for marginal stability as that in §3. The solution to the adjoint problem is shown in figure 7. Notice that $\tilde{w}$ is near zero in the liquid so that using the orthogonality condition (4.4) annihilates contributions from the liquid.

4.1. *Results*

Equation (4.5) contains two constants, $\bar{\tau}$ and λ, that are calculated in the weakly nonlinear analysis. The constant $\bar{\tau}$ can be calculated from linearized theory where complex growth rates are allowed. As discussed in Anderson & Worster (1995), the fact that $\bar{\tau} = 0$ for some choices of $\bar{S}$ and $\bar{C}$ indicates the presence of an oscillatory
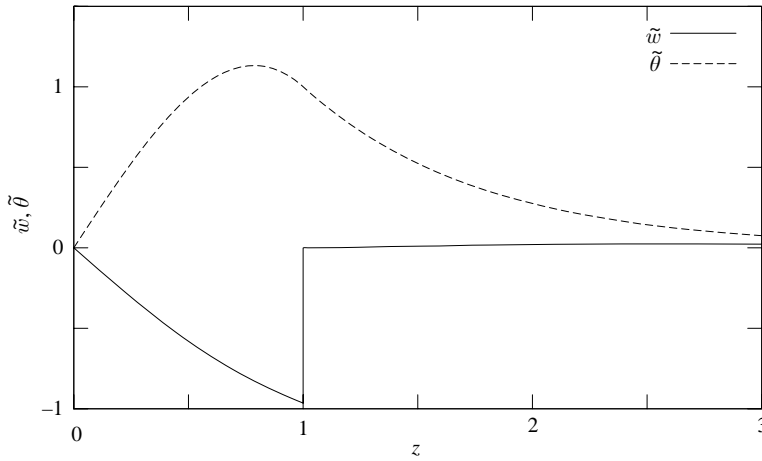
FIGURE 7. The adjoint solution, $\tilde{w}(z)$ and $\tilde{\theta}(z)$, for $\bar{S}=1$, $\bar{C}=1$ and $\sigma=2$, with $\mathscr{A}=0$.
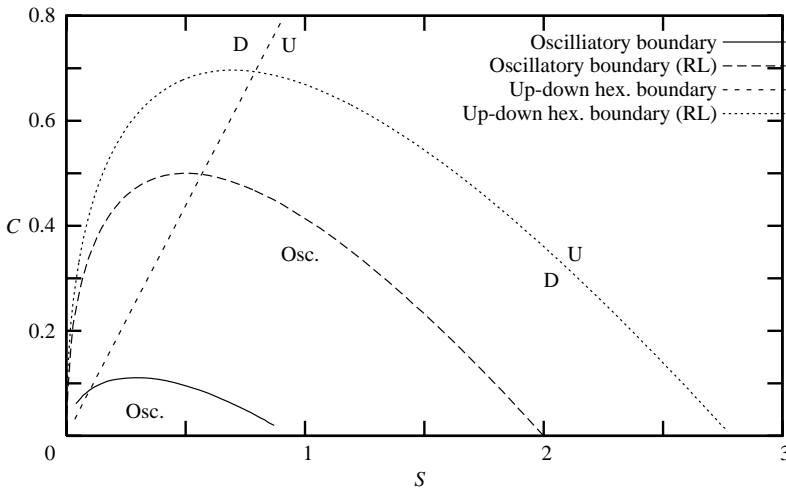

FIGURE 8. The location in S-C space where the coefficient of the time-dependent term changes sign, indicating the presence of an oscillatory instability (Anderson & Worster 1996). It also shows the boundary between the regions of parameter space in which up- or down-hexagons are stable, determined by the sign of b in (4.19). For the rigid-lid calculations, down-hexagons are preferred within the enclosed region; for the present analysis, down-hexagons are preferred to the left of the dashed line.

instability. There, $\bar{\tau}=0$ when

$$\frac{2\bar{S}}{(\bar{S}+\bar{C})^2} = 1. \tag{4.15}$$

Our analysis for the coupled two-layer problem reveals the presence of a similar oscillatory instability. Figure 8 shows the location of the $\bar{\tau}=0$ curve in $\bar{S}$-$\bar{C}$ parameter space. It has the same qualitative behaviour as the result of Anderson & Worster (1995), which is also plotted for comparison. The Landau constant λ is found to be approximately Λ/R^2, where Λ lies between about 46 and 52. As a result of our neglect of the effects of porosity variations by setting $\Pi(\chi)=1$, the bifurcation is
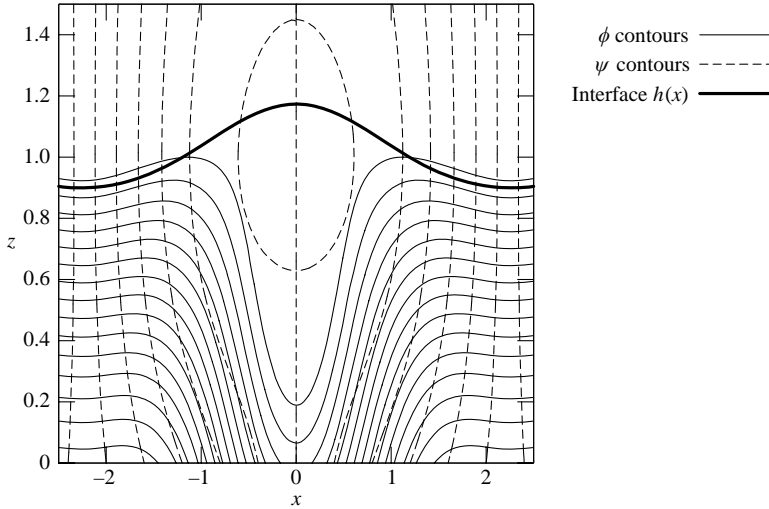
FIGURE 9. The solid fraction and streamlines for the case when $\delta = 0.25$, $\epsilon = 0.25$, $\mathscr{S} = 1$, $\mathscr{C} = 1$ and $\sigma = 1$ so that $\Omega = 2$. The contours of ϕ are shown in intervals of 0.05 starting at $\phi = 0$. The amplitude of the convection is large enough to have driven the solid fraction below zero in some parts of the mush.

always supercritical, $\lambda > 0$. The size of λ determines the amplitude as a function of the degree of supercriticality.

The finite-amplitude solutions, derived as a result of this analysis, show many common features with the full numerical solutions found by Schulze & Worster (1999). Where there is upflow, as a result of convection, the interface deflects upwards and the solid fraction is lowered. The point of minimum solid fraction is where the upflow in the linear solution is greatest, which from figure 6 is near the mush–liquid interface. In Amberg & Homsy (1993) and Anderson & Worster (1995), the maximum upflow, and therefore the birth of a chimney occurs deep in the mush, as a result of the impermeable mush–liquid interface. The streamlines and contours of the solid fraction in figure 9 show some qualitative agreement with the steady nonlinear solutions found by Schulze & Worster (1999), in the recirculating region the solid fraction has been driven below zero. In these finite-amplitude solutions, the chimney is born and grows from near the mush–liquid interface, unlike the solutions in Schulze & Worster (1999), but in agreement with the small $\mathscr{C}$ simulations of Chung & Chen (2000). Strictly speaking, limits of small $\mathscr{C}$ are not accessible in our analysis as we have written $\mathscr{C} = C/\delta$ with $C = O(1)$ as $\delta \to 0$. Chimneys are born and grow from the top of the mush because the greatest upflow is generated near the top of the mush in all parameter regimes under our assumptions that the mush interface is permeable and deformable.

4.2. Hexagonal patterns with $\mathscr{A} = 0$

The stability of hexagonal patterns can be studied by standard methods (Amberg & Homsy 1993; Anderson & Worster 1995; Chung & Chen 2000). We write all variables in terms of an unknown amplitude $A(\tau)$ so that, for example, the vertical velocity takes the form

$$ w = A(\tau)\bar{w}(z)\left[e^{ikx} + e^{ik(-x+\sqrt{3}y)/2} + e^{ik(-x-\sqrt{3}y)/2}\right] + \text{c.c.} \tag{4.16} $$
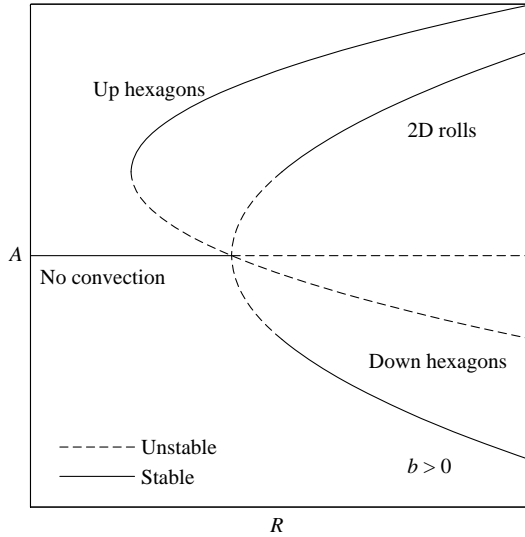
FIGURE 10. Sketch of the likely bifurcation structure in mushy-layer convection (from Anderson & Worster 1995). Whether up-hexagons or down-hexagons are stable depends on the sign of b. In the case shown here $b > 0$ and up-hexagons are stable. In the case where $b < 0$ down-hexagons are stable. The vertical axis represents the amplitude A and the horizontal axis the scaled Raleigh number R_1, the units are arbitrary.

When studying hexagonal planforms, the relevant expansion of the Rayleigh number and the time scale in terms of the small-amplitude parameter ϵ becomes

$$\delta R_m = R^2 + \epsilon R_1 + \cdots \qquad (4.17)$$

$$t = \epsilon \tau. \qquad (4.18)$$

The solution proceeds as usual and at $O(\epsilon^2)$ the compatibility condition yields the following amplitude equation

$$\bar{\tau} \frac{\mathrm{d}A}{\mathrm{d}\tau} = R_1 A + b\bar{A}^2 + \cdots. \qquad (4.19)$$

At $R_1 = 0$, the unstable branch of the hexagonal solutions intersects the $A = 0$ solution, which becomes unstable. Whether the up-hexagons or down-hexagons are stable or not is determined by the sign of b (figure 10). Our calculations show that to the left of the dashed line in figure 8, down-hexagons are the preferred form of the solution, in agreement with the experimental findings of Tait *et al.* (1992) (in which $\mathscr{C} = 12.3$ and $\mathscr{S} = 3.2$, predicting down-hexagons), although note that in those experiments $\mathscr{A} \neq 0$.

5. Conclusions

In this paper, we have seen that the limit $\theta_\infty \to \infty$ (correspondingly $\delta \to 0$) allows us to examine the structure of mushy-layer convection at onset in a straightforward way. We have relaxed the assumption of a rigid impermeable mush–liquid interface and found asymptotic solutions to the governing equations. We have determined the critical Rayleigh number and wavenumber for the case where the confining thermal buoyancy is negligible, $\mathscr{A} = 0$ and found that in this case the streamlines from convection penetrate through the mush–liquid interface and into the liquid layer above. In this case, the nonlinear development of the mushy layer leads to the

birth of a chimney much closer to the surface than in studies in which the rigid-lid approximation is used. We have also found solutions for a case when thermal buoyancy in the liquid is not negligible. In these cases, the thermal buoyancy acts to confine the convective motions in the mushy layer, and the results of the linear stability analysis are much closer to those derived from the rigid-lid results. A comparison of the linear stability results of Chung & Chen (2000) (in which the impermeability of the mush–liquid interface is relaxed, but the rigidity is maintained) shows that the inclusion of deformation in the mush–liquid interface leads to a further destabilization of the mushy layer relative to the case in which a constant-pressure boundary condition is used.

We have performed a weakly nonlinear analysis of cases when $\mathscr{A} = 0$ and found, in agreement with Chung & Chen (2000) that the chimney is born near the top of the mush. This is because the greatest upflow is predicted near the top of the mush when the rigid-lid assumption is abandoned. The analysis of hexagonal patterns predicts the boundary in parameter space at which up- and down-hexagons swap stability.

Although the rigid-lid assumption leads to a great simplification in the nonlinear analysis of convection, it may be possible to improve on the predictions made in such studies by using the asymptotic results presented here. It is hoped that this would lead to improved comparisons between experiment and theory or as a test of numerical schemes designed to model convection on mushy layers.

Appendix. Equations and boundary conditions at $O(\epsilon^2)$ and $O(\epsilon^3)$

The equations at order $O(\epsilon^2\delta^0)$ are

$$\bar{S}\frac{\partial \phi_{10}}{\partial z} + u_{00}\frac{\partial \theta_{00}}{\partial x} + w_{00}\frac{\partial \theta_{00}}{\partial z} + w_{10} = \nabla^2\theta_{10}, \tag{A 1}$$

$$-\bar{C}\frac{\partial \phi_{10}}{\partial z} + u_{00}\frac{\partial \theta_{00}}{\partial x} + w_{00}\frac{\partial \theta_{00}}{\partial z} + w_{10} = 0, \tag{A 2}$$

$$\nabla^2 w_{10} + R^2\frac{\partial^2\theta_{10}}{\partial x^2} = 0, \tag{A 3}$$

in the mush, and

$$w_{10} + u_{00}\frac{\partial \theta_{00}}{\partial x} + w_{00}\frac{\partial \theta_{00}}{\partial z} = \nabla^2\theta_{10}, \tag{A 4}$$

$$\nabla^4 w_{10} + \mathscr{H}\mathscr{A}R^2\delta^2\frac{\partial^2\theta_{10}}{\partial x^2} + \frac{\delta}{\sigma}\frac{\partial}{\partial z}\nabla^2 w_{10} = -\frac{1}{\sigma}\frac{\partial}{\partial x}\left(w_{00}\nabla^2 u_{00} - u_{00}\nabla^2 w_{00}\right), \tag{A 5}$$

in the liquid. The thermal boundary conditions are

$$\theta_{10} \to 0 \qquad \text{as } z \to \infty, \tag{A 6}$$

$$\theta_{10} = 0 \qquad \text{at } z = 0, \tag{A 7}$$

$$\theta_{10}(1^+) = \theta_{10}(1^-), \tag{A 8}$$

$$\left[\frac{\partial \theta_{10}}{\partial z} + h_{00}\frac{\partial^2\theta_{00}}{\partial z^2}\right]_{-}^{+} = 0, \tag{A 9}$$

$$h_{10} + \frac{\partial \theta_{00}}{\partial z}h_{00} + \theta_{10} = 0 \qquad \text{at } z = 1^+, \tag{A 10}$$

and the fluid-dynamical boundary conditions are

$$w_{10} \to 0 \qquad \text{as } z \to \infty, \tag{A 11}$$

$$w_{10}(1^+) + \frac{\partial w_{00}}{\partial z}(1^+)h_{00} = w_{10}(1^-) + \frac{\partial w_{00}}{\partial z}(1^-)h_{00}, \tag{A 12}$$

$$u_{10} + w_{00}\frac{\mathrm{d}h_{00}}{\mathrm{d}x} + \frac{\partial u_{00}}{\partial z}h_{00} = 0 \qquad \text{at } z = 1^+, \tag{A 13}$$

$$u_{10} + w_{00}\frac{\mathrm{d}h_{00}}{\mathrm{d}x} + \frac{\partial u_{00}}{\partial z}h_{00} = 0 \qquad \text{at } z = 1^-, \tag{A 14}$$

$$w_{10} = 0 \qquad \text{at } z = 0, \tag{A 15}$$

and finally, the boundary condition on the solid fraction is

$$\phi_{10}(1) = -h_{00}\frac{\partial \phi_{00}}{\partial z}(1). \tag{A 16}$$

The equations at $O(\epsilon^3 \delta^{-1})$ are

$$\frac{\partial \phi_{2(-1)}}{\partial z} = \frac{\partial \phi_{00}}{\partial \tau}, \tag{A 17}$$

and at $O(\epsilon^3 \delta^0)$, we have

$$\Omega\frac{\partial \theta_{00}}{\partial \tau} + \frac{\bar{S}}{\bar{C}}\phi_{2(-1)} + \Omega w_{20} + \Omega\left(u_{10}\frac{\partial \theta_{00}}{\partial x} + w_{10}\frac{\partial \theta_{00}}{\partial z} + u_{00}\frac{\partial \theta_{10}}{\partial x} + w_{00}\frac{\partial \theta_{10}}{\partial z}\right) = \nabla^2\theta_{20}, \tag{A 18}$$

$$\nabla^2 w_{20} + R^2\frac{\partial^2 \theta_{20}}{\partial x^2} + R_2\frac{\partial^2 \theta_{00}}{\partial x^2} = 0, \tag{A 19}$$

and in the liquid the equations are

$$\frac{\partial \theta_{00}}{\partial \tau} + w_{20} + u_{10}\frac{\partial \theta_{00}}{\partial x} + w_{10}\frac{\partial \theta_{00}}{\partial z} + u_{00}\frac{\partial \theta_{10}}{\partial x} + w_{00}\frac{\partial \theta_{10}}{\partial z} = \nabla^2\theta_{20}, \tag{A 20}$$

$$\frac{1}{\sigma}\left(\frac{\partial \nabla^2 w_{00}}{\partial \tau} - u_{00}\nabla^2 w_{10} + w_{00}\nabla^2 u_{10} + w_{10}\nabla^2 u_{00} - u_{10}\nabla^2 w_{00}\right) = -\nabla^4 w_{20}. \tag{A 21}$$

The appropriate thermal boundary conditions at this order are

$$\theta_{20} \to \infty \qquad \text{as } z \to \infty, \tag{A 22}$$

$$\theta_{20} = 0 \qquad \text{at } z = 0, \tag{A 23}$$

$$[\theta_{20}]_-^+ = \tfrac{1}{2}h_{00}^2[\theta_{00}'']_-^+, \tag{A 24}$$

$$\left[\frac{\partial \theta_{20}}{\partial z}\right]_-^+ = -\left[h_{00}\frac{\partial^2 \theta_{10}}{\partial z^2} + \frac{h_{00}^2}{2}\frac{\partial^3 \theta_{00}}{\partial z^3} + \frac{\partial^2 \theta_{00}}{\partial z^2}h_{10}\right]_-^+, \tag{A 25}$$

$$h_{20} = -\theta_{20} - \frac{\partial \theta_{10}}{\partial z}h_{00} - \frac{\partial \theta_{00}}{\partial z}h_{10} - \frac{\partial^2 \theta_{00}}{\partial z^2}h_{00}^2 \qquad \text{at } z = 1^+, \tag{A 26}$$

and the fluid-dynamical boundary conditions are

$$w_{20} \to \infty \qquad \text{as } z \to \infty, \tag{A 27}$$

$$[w_{20}]_-^+ = \left[-\frac{1}{2}\frac{\partial^2 w_{00}}{\partial z^2}h_{00}^2 + \frac{\mathrm{d}h_{00}}{\mathrm{d}x}u_{10} + \frac{\mathrm{d}h_{00}}{\mathrm{d}x}\frac{\partial u_{00}}{\partial z}h_{00} - h_{00}\frac{\partial w_{10}}{\partial z}\right]_-^+, \tag{A 28}$$

$$u_{20} = -\frac{\partial u_{00}}{\partial z}h_{10} - \frac{h_{00}^2}{2}\frac{\partial^2 u_{00}}{\partial z^2} - \frac{\partial u_{10}}{\partial z}h_{00} - w_{00}\frac{\mathrm{d}h_{10}}{\mathrm{d}x} - \left(w_{10} + \frac{\partial w_{00}}{\partial z}h_{00}\right)\frac{\mathrm{d}h_{00}}{\mathrm{d}x}, \tag{A 29}$$

$$w_{20} = 0 \qquad \text{at } z = 0. \tag{A 30}$$

Finally, the boundary condition for the solid fraction $\phi_{2(-1)}$ is

$$\phi_{2(-1)}(1^-) = 0. \tag{A 31}$$

REFERENCES

AMBERG, G. & HOMSY, G. M. 1993 Nonlinear analysis of buoyant convection in binary solidification with application to channel formation. *J. Fluid Mech.* **252**, 79–98.

ANDERSON, D. M. & WORSTER, M. G. 1995 Weakly nonlinear analysis of convection in mushy layers during the solidifcation of binary alloys. *J. Fluid. Mech* **302**, 307–331.

ANDERSON, D. M. & WORSTER, M. G. 1996 A new oscillatory instability in a mushy layer during the solidification of binary alloys. *J. Fluid Mech.* **307**, 245–267.

CHEN, F., LU, J. W. & CHANG, T. L. 1994 Convective instability in ammonium chloride solution directionally solidified from below. *J. Fluid Mech.* **276**, 163–187.

CHUNG, C. A. & CHEN, F. 2000 Onset of plume convection in mushy layers. *J. Fluid Mech.* **408**, 53–82.

CHUNG, C. A. & WORSTER, M. G. 2002 Steady-state chimneys in a mushy layer. *J. Fluid Mech.* **455**, 387–411.

FOWLER, A. C. 1985 The formation of freckles in binary alloys. *IMA J. Appl. Maths* **35**, 159–174.

GUBA, P. & WORSTER, M. G. 2006 Nonlinear oscillatory convection in mushy layers. *J. Fluid Mech.* **553**, 419–443.

HILLS, R. N., LOPER, D. E. & ROBERTS, P. H. 1983 A thermodynamically consistent model of a mushy zone. *Q. J. Mech. Appl. Maths* **36**, 505–539.

MULLINS, W. W. & SEKERKA, R. F. 1964 Stability of a planar interface during solidification of a binary alloy. *J. Appl. Phys.* **35**, 444–451.

RIAHI, D. N. 2002 On nonlinear convection in mushy layers. part 1. oscillatory modes of convection. *J. Fluid Mech.* **467**, 331–359.

SCHULZE, T. P. & WORSTER, M. G. 1999 Weak convection, liquid inclusions and the formation of chimneys in mushy layers. *J. Fluid Mech.* **388**, 197–215.

SCHULZE, T. P. & WORSTER, M. G. 2005 A time-dependent formulation of the mushy-zone free boundary problem. *J. Fluid Mech.* **541**, 193–202.

TAIT, S., JAHRLING, K. & JAUPART, C. 1992 The planform of compositional convection and chimney convection in a mushy layer. *Nature* **359**, 406–408.

WORSTER, M. G. 1986 Solidification of an alloy from a cooled boundary. *J. Fluid Mech.* **167**, 481–501.

WORSTER, M. G. 1992 Instabilities of the liquid and mushy regions during solidifcation of alloys. *J. Fluid Mech.* **237**, 649–669.

WORSTER, M. G. 1997 Convection in mushy layers. *Annu. Rev. Fluid Mech.* **29**, 91–122.